Dynamic Compensation of Harmonic, Sag and Interruption Using Unified Neural Network Controller with Levenberg-Marquardt Algorithm in Series Active Power Filter

Behzad Ghazanfarpour[1], Mohammad Reza Zare[2]
1- University Putra Malaysia, Electrical and Electronics Department, Malaysia
2- Center for Advanced Engineering Research, Majlesi Branch, Islamic Azad University, Isfahan, Iran
zareh81@gmail.com (Corresponding author)

Received: March 2015 Revised: June 2015 Accepted: June 2015

ABSTRACT:
This paper proposes a unified neural network controller in development of series active power filter. Three major power quality problems considered for this work are harmonics, sags, and interruptions, and dealing with all of them really needs effective unified algorithm which could adapt with variation of signals. Therefore, Levenberg-Marquardt (L-M) back propagation algorithm is introduced in this controller which helps the proposed controller to work properly with dynamic responses with appropriate achievement of convergence. Simulation results clearly show high performance of the proposed controller with series APF system. Its ability of adaptive estimating enhances the response time of the system to only one cycle. It performs well under various testing conditions with significant reduction of harmonics, correction of sags, and fast response to interruptions.

KEYWORDS: Sags, Harmonics, Interruptions, Neural Network, Active Power Filter, Power Quality

1. INTRODUCTION

Efficient, reliable and quality electrical power supply is paramount for the growth of an industrial plant. Rising number of sensitive digital devices and informatics applications in nowadays industries has made the quality of transmitted power to a serious concern[1]. The term "power quality" is investigated from the aspects of reliability of supply and quality of transmitted power [2-4]. In general, operating loads without disturbing or damaging them by utility is interpreted as the reliability of supply. Therefore, quality of voltage at point of common coupling (PCC) could be a main concern of a consumer [5-6]. Voltage quality at PCC is regularly evaluated as resultant of the effects of all upstream suppliers. Of course it should be noted that voltage quality and current quality affect each other through system and load impedances[7]. The most pressing voltage quality issues at PCC are voltage sags, interruptions and power system harmonics [5, 8]. These mentioned problems have considerable effect to not only on technological site but may affect economical site too[9]. Voltage sag is a momentary drop at fundamental frequency in range of 0.1 p.u to 0.9 p.u at rms voltage of line and can last from 0.5 cycle to 1 minute. Practically, abrupt increases in loads such as short circuits, faults, motor starting and power factor correction capacitors are lead to abrupt increases in source impedances that lead to voltage sag [10]. Referring to Bell's Lab surveys in this area, momentary voltage sags constitute 87% of power quality problems especially in low voltage systems[8]. Interruption is the drop in supply voltage to below 0.1 p.u for a time period of not exceeding 1 minute. In general, due to delaying in protective devices and voltage sag may proceed to interruptions on the source system[7]. Voltage quality problems such as sags and interruptions are sorted as short-term events. Power system harmonics are the type of power quality problems that tend to occur in much longer intervals than sags and interruptions. Typically occurrence of harmonics is caused by applied nonlinear devices in distribution system[11]. Harmonic sources like transformers, rotating motors and arc furnaces are classified as conventional type of nonlinear devices. In addition to conventional nonlinear devices, power electronic devices are also categorized as harmonic generators over the past years. Extensive usage of nonlinear devices such as static rectifiers, adjustable speed drives, HVDC transmission and switch mode power supplies are leading to distortion of voltage and current signals

waveforms[12]. In term of voltage quality at PCC harmonics are the major reasons to make voltage waveforms of the supply distorted. Voltage distortion can cause severe device malfunction and failure which is commonly remarked as load disruption. Moreover, equipment losses have been increasing due to the effect of harmonics which is known as the thermal stress[13]. Harmonics are broadly interpreted as the sinusoidal voltages or currents with frequencies which are integer multiples of operational frequency of supply system [14-15]. Increasing of power consumer interactions in distribution system and awareness of power costs will emphasize on local compensation.

An integrated fast local compensation is able to create a constant power for loads. Active power filters (APFs) have been introduced as a superior solution for power quality issues[16-17]. Utilization of APFs can improve power factor correction of system as well as harmonics elimination [12]. Majority of researches have determined series configuration of APF as the most effective way for compensating of voltage deregulations and distortions at the PCC [12], [18]. Section II in this paper is dedicated to the circuit configuration and principle of the series APF. Performance and effectiveness of an APF principally depends on its controller. Thus, designing a reliable and integrated controller is a serious concern of this research area. The controller can keep the load side voltage constant without adding any risk to the system stability factors. In this work, the proposed compensator system employs a unified neural network controller. Earlier research works have proved effectiveness of neural network techniques in controlling nonlinear system [19-21].

The main advantage of neural network over the other techniques is its ability of online adaptation. Thus, the controller is able to extract different changes of a non-linear system and adapt to its variation in real time [22]. In this work, a feed-forward neural network controller based on Levenberg-Marquardt (L-M) algorithm is proposed. Previous research works have broadly used Widrow-Hoff (W-H) algorithm to train feed-forward neural networks. Basically, neural network is applied to controller of the series APF to extract utility line signal at the fundamental frequency (which can be 50 or 60 Hz). W-H based controllers are regularly suitable for harmonic compensating conditions due to less variations of the utility line signal especially in term of its magnitude. Practically, in W-H weight updating algorithm, a constant learning rate is chosen [23-26]. This constant value makes W-H training algorithm unable to converge to the variation of the signal. In addition to its inaccurate convergence, the constant learning rate slows down the system performance. Sags and interruptions are classified as sort of problems which are more engaged with dynamic change in the magnitude of the signal.

Unlike W-H algorithm, the proposed L-M algorithm is very suited to detect variations in both magnitude and phase angle of the signal. The Levenberg–Marquardt (L-M) algorithm blends the steepest descent method and the Gauss–Newton algorithm. Thus, it inherits the speed advantage in addition to the robustness [27]. Therefore, L-M algorithm is the modified type of those algorithms that can approximate the minimum error in each iteration. Indeed, L-M algorithm includes a parameter of combination coefficient μ (with step 1/μ) in its learning rate calculation. It is used as an optimizing parameter in learning rate of L-M algorithm [28-29].

After Section 2, section 3 covers the development and analysis of the proposed unified controller. Results are presented in section 4 and section 5 concludes the work.

2. PRINCIPLE OF SERIES APF

Series APFs broadly consist of two main units: compensator and controller [12]. The configuration of series APF is covered in this section. In series APF, the compensator unit mainly includes four main operative parts [16]:

1) A voltage source inverter (VSI) with IGBT switches which is operated by pulse width modulation (PWM). Output signal of controller unit is the reference signal for the APF.

2) A DC supply for the VSI. In this work a rechargeable battery is considered as the supply source in order to generate proper compensating voltage. The implemented battery is charged by the utility line.

3) A second order low-pass LC filter is designed to make the output voltage of inverter in sinusoidal waveforms and to absorb high frequency switching noises. Besides duplicating the reference signal of the PWM, the VSI also generates some other higher-order harmonics. The transfer function of the low-pass filter is given by:

$$\frac{V_{inj}}{V_{inv}} = \frac{1}{S^2LC+1} \quad (1)$$

4) A transformer that connects the APF with the power line in series. In this work, a linear transformer with winding ratio of 1:1 is applied. This transformer may be used as the protection for the applied filter.

Figure (1) shows configuration of the series APF. Furthermore, to prepare compensating voltage, calculating the value of voltage sag is a need. Voltage supply V_o with connection of the series APF is:

$$V_o = V_s + V_c \quad (2)$$

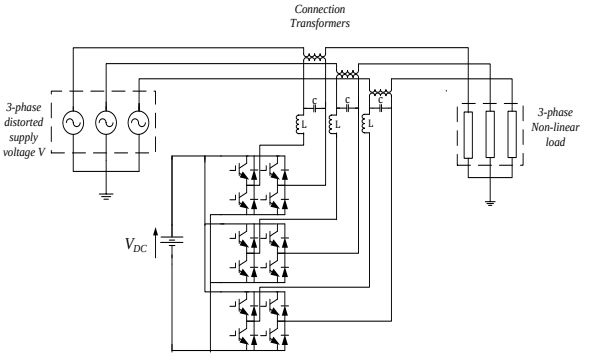

Fig. 1. Configuration of three-phase series APF

Where V_s is the utility grid voltage and V_c is the compensation voltage produced by the series APF.
It is noticed that at normal condition, V_c is zero and V_o is equal to V_s For control purposes, a reference signal V_{ref} is considered as the desired load side voltage; and in the normal condition the value of V_{ref} is equal to V_s . During the voltage sag, utility voltage is obtained from equation below:

$$V_s = (1-s)\ \ V_{ref} \tag{3}$$

Where S represents the amount of voltage drop in magnitude per unit. Therefore, during the occurrence of interruption, equations (2) and (3) can also be considered. Note that, sag and interruption conditions can cause phase angle shifting [30-31]. Thus, for synchronizing V_{ref} with the new phase angle, a phased locked loop (PLL) system is considered [32]. This part is discussed in detail in section III. Furthermore, to compensate the present harmonics at the distorted voltage source at PCC, the supply voltage V_s is modeled as below:

$$V_s = V_{fund}\sin\omega t + \sum_{h=3,5,7,\ldots}^{\infty} V_h \sin(h\omega t - \phi_h) \tag{4}$$

Where V_s is the measured voltage of the distorted voltage supply that contains V_{fund} as the fundamental voltage component of the utility line and V_h as the voltage harmonic components and ϕ_h represents the phase angle of harmonic order. Therefore, to obtain constant and clean sinusoidal load side voltage V_L , series APF needs to produce and inject voltage V_{inj} equal to voltage harmonics. It could be explained as follow:

$$V_L + V_{inj} = V_{fund}\sin\omega t + \sum_{h=3,5,7,\ldots}^{\infty} V_h \sin(h\omega t - \phi_h) \tag{5}$$

To generate the desired compensating voltage V_{inj} ,the controller extracts harmonic voltage components V_h at the utility line voltage. This extracted signal is compared with the triangular wave to produce PWM switching signals to the gates of the VSI. The output of the VSI is passed through a LC low-pass filter so that V_{inj} consists of only the desired compensating voltages.
Circuit block diagram of the proposed dynamic compensation approach for voltage sag and harmonics is shown in figure (2).

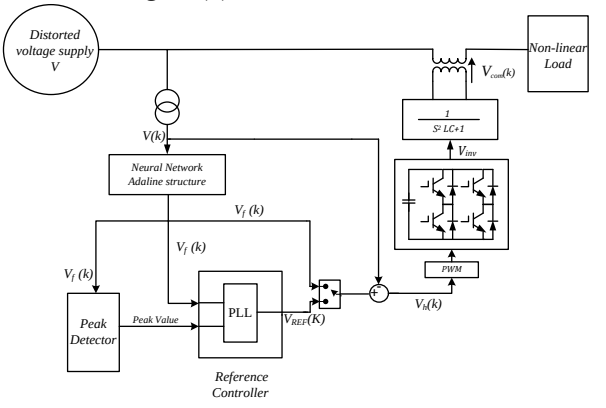

Fig. 2. Block diagram of proposed series APF

3. UNIFIED NEURAL NETWORK CONTROLLER ARCHITECTURE

In the Fourier series theory, any periodic signal can be represented by the sum of sine and cosine components with a suitable coefficient attached to each of these components [33-34]. Through this concept, the voltage signal of the utility system at the PCC can be modeled as:

$$V(t) = \sum_{n=1,2,3}^{N} w_{an}\sin(n\omega t) + w_{bn}\cos(n\omega t) \tag{6}$$

Where amplitudes of the sine and cosine components of the supply voltage V are w_{an} and w_{bn} respectively. Moreover, n represents the order of harmonic in which N is defined as the last order of the measured harmonics.
This concept brings the designed controller to have three main parts as will be discussed further. The configuration of the proposed controller is also depicted in figure (2).

3.1. Neural Network Unit Principle and Architecture

In this work, a feed-forward neural network based structure is exploited as the basis of the proposed approach. The goal is to estimate present harmonic components of utility line voltage. The conventional type of neural network based controller extracts distortion components while its output signal is the fundamental signal of the supply line voltage. Hence, the calculation process is complex and time consuming. Therefore, to enhance the system performance the

proposed controller is designed to detect and estimate the nominal voltage signal of supply. This estimation needs to have a stable convergence to the signal fluctuation in addition to speed. Thus, the proposed training algorithm for neural network is Levenberg-Marquardt (L-M) algorithm. The proposed training algorithm is applied at the ADALINE structure of neural network. Basically, ADALINE is suitable to be utilized as fundamental signal processor since it has only two inputs and one output. Its structure is shown in figure (3).

Figure (3) and equation (6), only two weight elements of fundamental components need to be updated. This idea is based on orthogonal relationship between vector $\overline{X}(k)$ elements. The difference between the actual value of fundamental components of measured *V(k)* and estimated value $V_{est}(k)$ is interpreted as the error *e(k)*.

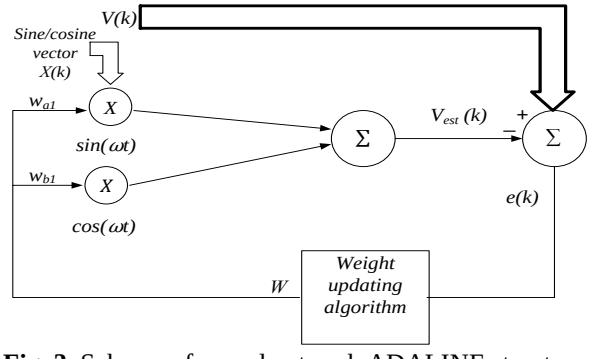

Fig. 3. Scheme of neural network ADALINE structure

$$\overline{X}(k)=\begin{bmatrix}\sin(k\omega\Delta t)\\ \cos(k\omega\Delta t)\end{bmatrix} \tag{7}$$

and

$$\overline{W}(k)=[w_{a1},w_{b1}] \tag{8}$$

Where $\overline{W}(k)$ is a set of weights in each iteration in matrix form as shown in equation (8). Therefore, to minimize the value of *e(k)*, an update rule for $\overline{W}(k)$ should be interpreted while the output of the neural network is calculated as below:

$$V_{est}(k)=w_{a1}\sin(k\omega\Delta t)+w_{a2}\cos(k\omega\Delta t) \tag{9}$$

The proposed weight updating algorithm for $\overline{W}(k)$ is based on L-M back propagation algorithm. L-M is the modified type Gauss-Newton method while back propagation is a steepest descent algorithm. Updating algorithm of Gauss-Newton is presented as follow [27], [35]:

$$\overline{W}(k+1)=\overline{W}(k)+\left(\overline{J}^{T}(k)\overline{J}(k)\right)^{-1}\overline{J}(k)e(k) \tag{10}$$

Where *e(k)* is the sum of squares error (SSE) and can be calculated as follow:

$$SSE=\sum_{i=1}^{n}e_i^2(k) \tag{11}$$

n is the number of neural network structure output. Also, from equations (6), (8) and (11) the Jacobian matrix *J(k)* can be shown as:

$$\overline{J}(k)=\begin{bmatrix}\frac{\partial e_1}{\partial w_{a1}} & \frac{\partial e_1}{\partial w_{b1}}\end{bmatrix} \tag{12}$$

Therefore, from equations (7) and (9) the derived Jacobian matrix can be rewritten as:

$$\overline{J}(k)=\begin{bmatrix}\sin(k\omega\Delta t) & \cos(k\omega\Delta t)\end{bmatrix}=\overline{X}^{T}(k) \tag{13}$$

The relationship between Jacobian matrix *J* and Hessian matrix *H* can be considered as below[35]:

$$\overline{H}\approx\overline{J}^{T}\overline{J} \tag{14}$$

The Gauss-Newton algorithm is facing a convergence problem to optimize complex errors; since mathematically, matrix J^TJ may not be invertible. Therefore, to make the approximated Hessian matrix J^TJ invertible, another approximation to the Hessian matrix is proposed by L-M algorithm[28].

$$\overline{H}\approx\overline{J}^{T}\overline{J}+\mu I \tag{15}$$

Where μ is always positive and called combination coefficient and I is identity matrix.

Hence, from equation (15), it can be noticed that the hessian matrix is always invertible since the elements of its main diagonal are larger than zero.

Therefore, through combination of equations (10) and (15) the updating rule of L-M algorithm can be written as below[35]:

$$\overline{W}(k+1)=\overline{W}(k)+\left(\overline{J}^{T}(k)\overline{J}(k)+\mu I\right)^{-1}\overline{J}(k)e(k) \tag{16}$$

Thus, from equations (13) and (16), the implemented weight updating algorithm based on L-M algorithm concept is derived as follow:

$$\overline{W}(k+1)=\overline{W}(k)+\left(\overline{X}(k)\overline{X}^{T}(k)+\mu I\right)^{-1}\overline{X}^{T}(k)e(k) \tag{17}$$

With the Levenberg–Marquardt weight updating algorithm and the computation of Jacobian matrix, the next step is to organize the training process. The key factor for optimizing the training process is the combination coefficient parameter μ. From equation (17), it is inferred that variations of parameter μ is

directly related to the value changing of error function e(k). The step size of combination coefficient in each iteration is 1/μ. Therefore, if e(k) keeps increasing in each iteration, it implies that μ could change to larger value by multiplying to some factor β (β >1). This procedure continues until the system reaches to the least value of e(k). On the other hand, parameter μ is divided by β to speed up the system while e(k) keeps reducing in each iteration.

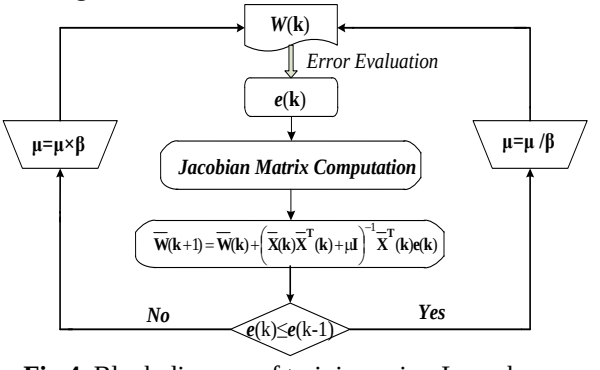

Fig.4. Block diagram of training using Levenberg-Marquardt algorithm

3.2. Peak Detector Unit

The second part of the controller unit is the peak value detector. It receives output signal of the ADALINE to calculate the peak value of the fundamental signal. In this part, with concept of fast Fourier transform, the received signal is transferred from time domain to frequency domain. The peak amplitude value is memorized by the peak detector at the steady state by using a MATLAB S-function. The memorized value has two roles. First, it is utilized as the amplitude determiner for the reference controller. Second, it is used to compare continuously with amplitude values of the fundamental signal of power line and load side voltage. This comparison is used to determine magnitude of voltage drop at fundamental frequency.

3.3. Reference Controller Unit

In this part, the reference controller unit is covered. This unit generates a controlling signal to operate the compensator unit of series APF during the under-voltage conditions. Note that phase shifting is also a characteristic of sag as well as voltage drop. Therefore, the reference controller utilizes a phase locked loop (PLL) control system. PLL basically consists of a variable frequency oscillator and a phase detector. It operates to match the phase of the generated reference signal with phase angle variations of utility line signal by adjusting its oscillating frequency. This oscillator is technically a zero detector. Consequently, PLL frequency synchronization can be confronted by malfunction due to the presence of harmonics. Thus to enhance the performance of the reference controller, its input is taken from the neural network structure. On the other hand, the output signal of PLL has the constant magnitude of one. Hence, it is multiplied by the calculated peak value of the peak detector to achieve desired reference signal. Thereupon, with the generated reference signal, the series APF is able to compensate under-voltage conditions and keep the grid nominal voltage constant and synchronized.

4. RESULTS AND DISCUSSION

In this section, the results are covered. First, the results of the proposed neural network controlling system are discussed. The proposed approach performs an accurate convergence to the extracted signal with approximation error of $3x10^{-3}$. Furthermore, its ability of adaptive estimating enhances the response time of the system to only one cycle. Figure (5) shows the estimating of utility line voltage fluctuations by Levenberg-Marquardt (L-M) algorithm. The updating value of combination coefficient of L-M training is depicted in figure (6).

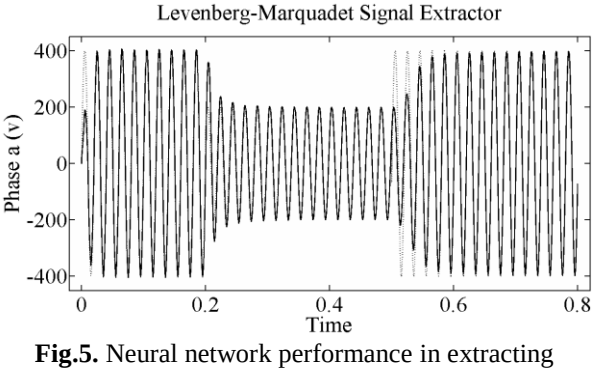

Fig.5. Neural network performance in extracting nominal voltage signal fluctuations

The simulation works were performed by using MATLAB-Simulink tool. The testing was carried out on the 20kVA three-phase system with 400 V peak. The planned system contains a three-phase distorted voltage supply at PCC, a three-phase series APF with the proposed unified neural network controller.

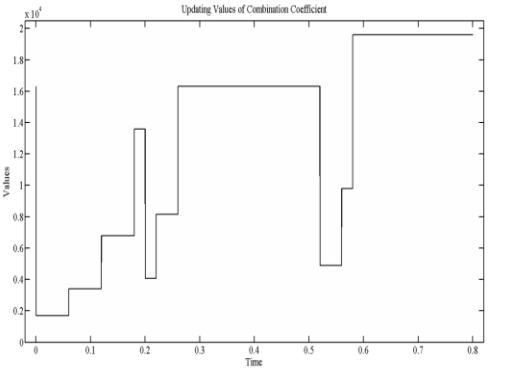

Fig.6. The updating value of parameter **μ** during variation of nominal voltage signal

The simulated conditions considered from where the line voltage distortion at the PCC was induced as a result of the reactive nature of other loads connected to the PCC. Two cases of power quality problems were took under study in this article. The first case contains of balanced voltage harmonic and sag associated with unbalanced voltage sag, while the second case assigned to the conditions of unbalanced voltage harmonic and sag occurrence at the voltage supply. The simulation of first case study took place under the following conditions. At the first step, all three phases were subjected to the same total harmonic distortion (THD) value. In the second step, balanced three-phase sag condition with phase angle shifting occurred on the supply side voltage at PCC. Then an unbalanced harmonic distortion was applied on the utility line voltage at the PCC in the third step. These three steps in source side voltage fluctuations depicted in figure (7).

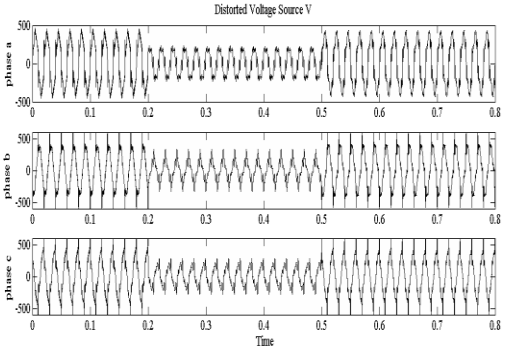

Fig.7. Waveforms of distorted three-phase voltage supply for phases (a), (b) and (c)

In the first simulation testing (for $0 \leq t < 0.2s$), the supply was subjected to three-phase balanced harmonics.

Table (1) shows the magnitude and phase angle of the 29^{th} order of the present harmonics in this test. The supply at this stage was remarkably distorted with total harmonic distortion (THD) of 24.8% at each phase.

Table 1 Three phase balanced harmonic orders and values

	Phase a		Phase b		Phase c	
Order	Amp. (V)	Ang (°)	Amp. (V)	Ang (°)	Amp. (V)	Ang (°)
Fundamental	400	0	400	-120	400	120
3	23	-43	23	120	23	-43
5	52	-37	52	-43	52	-163.
7	24	20	24	83	24	157
9	37	51	37	-97	37	140
11	29	47	29	100	29	51
13	33	23	33	51	33	-17
15	21	33	21	73	21	167
17	20	15	20	-143	20	97
19	26	43.5	26	143	19	33
21	16	29	16	33	16	-15
23	25	25	25	135	25	105
25	22	66	22	-97	22	163.
27	17	-40	17	76.5	17	5
29	15	-80	15	29	15	29
				145		-95
				-54		186
				-40		-40
				40		-200

The precise signal tracking by the controller, as can be seen in figure (5), contributes series APF to reduce the THD down to 0.7% on each phase. Furthermore, the speed of system in dynamic compensating is notably enhanced by the proposed neural network controller. This capability is more significant in compensating short term faults like voltage sag. In the second stage (for $0.2s \leq t < 0.5s$), three-phase balanced sag with 50% voltage drop and 30° phase angle shifting were applied at each phase. This sag condition was simulated as result of starting up of a faulty three-phase motor. Thus, power system harmonics with THD of 28% at each phase are also observed along with voltage sag. Figure (8) as an operation sample of the proposed system reveals the compensation of harmonics and voltage sag at the third phase of the supply (phase (b) with -120° phase angle). The obtained results from figures (5) and (8) determines that after only half cycle system is able to perfectly compensate harmonics and sags.

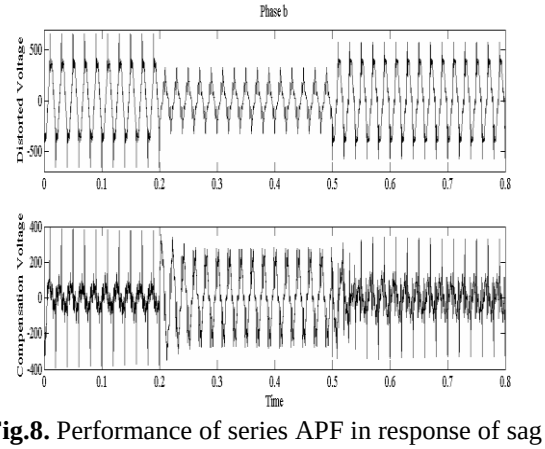

Fig.8. Performance of series APF in response of sag and harmonic for phase (b)

The measured THD after the compensation was 0.8% at each of the phases with an unnoticeable effect of phase shifting at the load side. On the other hand, at the third stage (for $0.5s \leq t$), three-phase unbalanced harmonic with -40° phase shifting was applied at the supply at PCC.

The phase shifting was determined due to the nature of nonlinear loads linked to a same PCC. The measured

THD at this stage was 89% and 21th order of odd harmonics observed as can be referred to Table (2).

Table 2 Three phase unbalanced harmonic orders and values

	Phase a		Phase b		Phase c	
Order	Amp. (V)	Ang (°)	Amp. (V)	Ang (°)	Amp. (V)	Ang (°)
Fundamental	400	0	400	-120	400	120
3	35	42	32	36.5	40	-22
5	44	-28	45	140	60	199
7	33	-5	33	-111	33	171
9	42	54	60	78	40	16.5
11	22	71	32	134	25	-100
13	22	10	55	-99	24	203
15	33	-12	25	23	30	55
17	28	-17	33	143	29	-92
19	14	14	17	-83	27	137
21	18	-7	21	45	23.5	45

The resultant waveforms in figure (9) clearly show that the series APF is able to adapt instantly with the variation of distortions. The THD was reduced to 2.6% as the result of the high compensating ability of the proposed series APF. Furthermore, simultaneously convergence of the system output with the variation of the utility line signal leads to keep the robustness of compensating process. Therefore, from figure (9), it can be observed that the adverse effect of voltage sag at the load side voltage is negligible.

Figure (10) shows an unbalanced three-phase sag condition (for 0.2s≤ t< 0.5s) at utility supply at PCC. Unbalanced sag condition can be caused by implementation of adjustable speed drive. The simulated work was done by using controllable voltage supply. The capability of the proposed series APF in dynamic compensating of three different voltage drop condition was evaluated. From figure (10), it can be observed that phases (a) and (c) subjected to an unbalanced poly-phase sag condition at the PCC.

The observed sag condition caused 40% and 25% voltage drop with 45° phase shifting to phases (a) and (c) respectively. Furthermore, phases (a) and (c) also faced harmonic distortion with THD of 36% and 30% during sag respectively. On the other hand, while poly-phase sag on phases (a) and (c), 95% of voltage drop caused a single phase interruption to phase (b). The corresponding response of the proposed series APF to this condition can be shown in figures (11), (12) and (13). The fast and robust detection of faults on the supply leads to generate three different values of duty cycle by the series APF. Thereupon, from obtained results it can be perceived the series APF generates proper dispensed compensation for each phase.

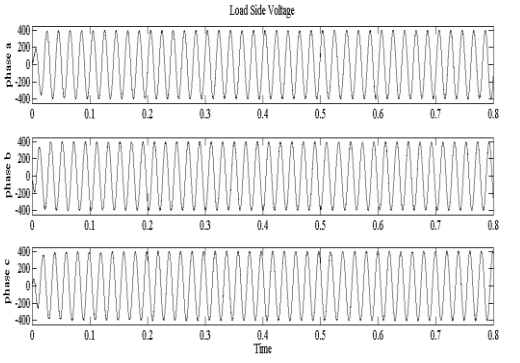

Fig.9. Waveforms of load side voltage for phases (a), (b) and (c) respectively

In the second case study, the voltage supply was subjected to an unbalanced three phase voltage sag associated with a single phase interruption and harmonic distortion. This test was done to verify the capability of the proposed system in regulating the voltage source. The observed variation of the utility supply during the unbalance sags and interruption is shown figure (10).

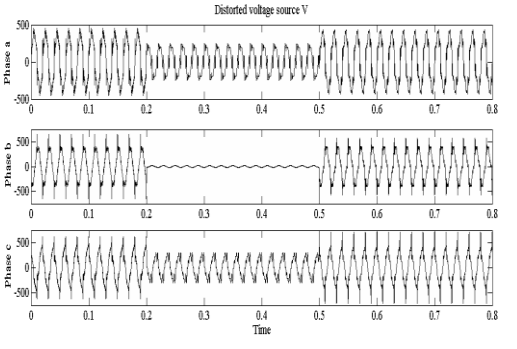

Fig.10. Waveforms of supply voltage while harmonic and unbalanced under-voltage

The acquired results of this special case demonstrate the effectiveness of the proposed system. In addition, the compensation process causes no tangible voltage transients at the load side voltage.

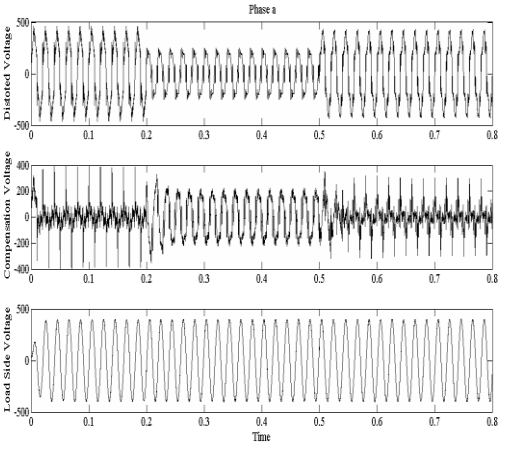

Fig. 11. Waveforms of supply, compensation and load side voltage respectively for phase (a)

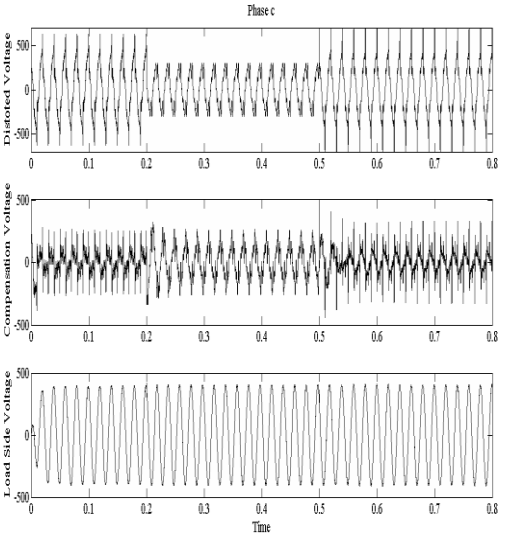

Fig.12. Waveforms of supply, compensation and load side voltage respectively for phase (c)

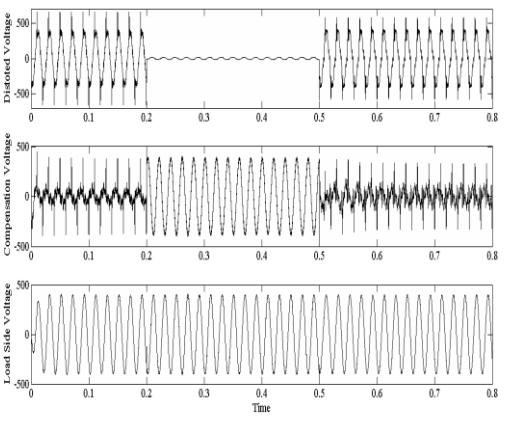

Fig.13. Waveforms of supply, compensation and load side voltage respectively for phase (b)

5. CONCLUSION

In this work, a new voltage compensator for power system harmonics, voltage sag and interruption has been proposed. The proposed system utilizes a series APF with a unified neural network controller. The basis of the controller is Levenberg-Marquardt (L-M) backpropagation technique. The applied neural network algorithm enhances system performance and accuracy of convergence to the nominal voltage signal. The simulations results demonstrate its proficiency for powering load under different under-voltage conditions and harmonics. The proposed series APF is able to keep the load side voltage constantly equal to nominal voltage and clearly sinusoidal. Finally, the proposed series APF is proven to be able to compensate the voltage grid faults and distortions at PCC without adding any risk to the system stability factors. Its ability helps to maintain quality of end user power requirements.

REFERENCES

[1] M. McGranaghan and B. Roettger, **"Economic evaluation of power quality,"** *Power Engineering Review, IEEE,* Vol. 22, pp. 8-12, 2002.

[2] M. Bollen, **"What is power quality?,"** *Electric Power Systems Research,* Col. 66, pp. 5-14, 2003.

[3] A. Kannan, *et al.*, **"A review of power quality standards, electrical software tools, issues and solutions,"** in *Renewable Energy and Sustainable Energy (ICRESE), 2013 International Conference on*, 2013, pp. 91-97.

[4] M. Torabian Esfahani and B. Vahidi, **"A Novel Delay-less Control of Unified Power Quality Conditioner to Enhance Power Quality in Power System,"** *Electric Power Components and Systems,* Vol. 42, pp. 1776-1791, 2014/12/10 2014.

[5] J. Arrillaga, *et al.*, **"Power quality following deregulation,"** *Proceedings of the IEEE,* Vol. 88, pp. 246-261, 2000.

[6] B. K. Perera, *et al.*, "**Point of common coupling (PCC) voltage control of a grid-connected solar photovoltaic (PV) system,"** in *Industrial Electronics Society, IECON 2013 - 39th Annual Conference of the IEEE*, 2013, pp. 7475-7480.

[7] R. C. Ducan, *et al.*, **"Electrical power system quality,"** ed: McGraw-Hill, 2002.

[8] K. Gulez, **"Neural network based switching control of AC–AC converter with DC–AC inverter for voltage sags, harmonics and EMI reduction using hybrid filter topology,"** *Simulation Modelling Practice and Theory,* Vol. 16, pp. 597-612, 2008.

[9] J. V. Milanovic and C. P. Gupta, **"Probabilistic assessment of financial losses due to interruptions and voltage sags-part I: the methodology,"** *Power Delivery, IEEE Transactions on,* Vol. 21, pp. 918-924, 2006.

[10] M. F. Alves and T. N. Ribeiro, **"Voltage sag: an overview of IEC and IEEE standards and application criteria,"** in *Transmission and*

Distribution Conference, 1999 IEEE, Vol. 2, pp. 585-589, 1999.

[11] F. Z. Peng and D. J. Adams, **"Harmonic sources and filtering approaches-series/parallel, active/passive, and their combined power filters,"** in *Industry Applications Conference, 1999. Thirty-Fourth IAS Annual Meeting. Conference Record of the 1999 IEEE*, Vol. 1, pp. 448-455, 1999.

[12] H. Akagi, **"Active Harmonic Filters,"** *Proceedings of the IEEE*, Vol. 93, pp. 2128-2141, 2005.

[13] J. Arrillaga and N. R. Watson, *Power System Harmonics*: Wiley, 2003.

[14] **"IEEE Guide for Application and Specification of Harmonic Filters,"** *IEEE Std 1531-2003*, pp. 0_1-60, 2003.

[15] S. B. Efe, **"Harmonic filter application for an industrial installation,"** in *Engineering of Modern Electric Systems (EMES), 2015 13th International Conference on*, 2015, pp. 1-4.

[16] M. El-Habrouk, *et al.*, **"Active power filters: a review,"** *Electric Power Applications, IEE Proceedings* -, vol. 147, pp. 403-413, 2000.

[17] K. Steela and B. S. Rajpurohit, "A survey on active power filters control strategies," in *Power Electronics (IICPE), 2014 IEEE 6th India International Conference on*, 2014, pp. 1-6.

[18] A. Emadi, *et al.*, *Uninterruptible Power Supplies and Active Filters*: Taylor & Francis, 2004.

[19] W. Anis Ibrahim and M. M. Morcos, **"Artificial intelligence and advanced mathematical tools for power quality applications: a survey,"** *Power Delivery, IEEE Transactions on*, Vol. 17, pp. 668-673, 2002.

[20] T. C. Green and J. H. Marks, **"Control techniques for active power filters,"** *Electric Power Applications, IEE Proceedings* -, Vol. 152, pp. 369-381, 2005.

[21] L. Saribulut, *et al.*, **"Artificial neural network-based discrete-fuzzy logic controlled active power filter,"** *Power Electronics, IET*, Vol. 7, pp. 1536-1546, 2014.

[22] P. J. Werbos, **"An overview of neural networks for control,"** *Control Systems, IEEE*, Vol. 11, pp. 40-41, 1991.

[23] M. A. M. Radzi and N. A. Rahim, **"Neural Network and Bandless Hysteresis Approach to Control Switched Capacitor Active Power Filter for Reduction of Harmonics,"** *Industrial Electronics, IEEE Transactions on*, Vol. 56, pp. 1477-1484, 2009.

[24] A. Djaffar Ould, *et al.*, **"A Unified Artificial Neural Network Architecture for Active Power Filters,"** *Industrial Electronics, IEEE Transactions on*, Vol. 54, pp. 61-76, 2007.

[25] L. H. Tey, *et al.*, **"Adaptive neural network control of active filters,"** *Electric Power Systems Research*, Vol. 74, pp. 37-56, 2005.

[26] S. Bangia, *et al.*, **"Design of dIstributed Active Filters using neural network for the enhancement of power quality,"** in *Advance Computing Conference (IACC), 2013 IEEE 3rd International*, 2013, pp. 626-630.

[27] H. Yu and B. Wilamowski, **"Levenberg-Marquardt Training,"** *The Industrial Electronics Handbook*, Vol. 5.

[28] L. S. H. Ngia and J. Sjoberg, **"Efficient training of neural nets for nonlinear adaptive filtering using a recursive Levenberg-Marquardt algorithm,"** *Signal Processing, IEEE Transactions on*, Vol. 48, pp. 1915-1927, 2000.

[29] J. More, **"The Levenberg-Marquardt algorithm: implementation and theory,"** *Numerical analysis*, pp. 105-116, 1978.

[30] M. H. J. Bollen, **"Characterisation of voltage sags experienced by three-phase adjustable-speed drives,"** *Power Delivery, IEEE Transactions on*, Vol. 12, pp. 1666-1671, 1997.

[31] E. C. Aeloiza, *et al.*, **"Analysis and design of a new voltage sag compensator for critical loads in electrical power distribution systems,"** *Industry Applications, IEEE Transactions on*, Vol. 39, pp. 1143-1150, 2003.

[32] R. Best and P. L. Loops, **"Design, Simulation, and Applications. 2003,"** ed: McGraw-Hill, New York.

[33] M. H. Bollen and I. Gu, *Signal processing of power quality disturbances* vol. 30: Wiley-IEEE Press, 2006.

[34] P. V. O'Neil, *Advanced Engineering Mathematics*: Nelson Education Limited, 2011.

[35] M. T. Hagan and M. B. Menhaj, **"Training feedforward networks with the Marquardt algorithm,"** *Neural Networks, IEEE Transactions on*, Vol. 5, pp. 989-993, 1994.